



<b>Publication Year</b>	2018
<b>Acceptance in OA</b>	2020-11-05T16:43:41Z
<b>Title</b>	WEAVE spectrograph cameras: the polishing of the spherical lenses
<b>Authors</b>	Izazaga, Rafael, Carrasco, Esperanza, Hidalgo, Andrea, Aguirre, Daniel, Terlevich, Elena, Terlevich, Roberto, Dalton, Gavin, Trager, Scott, Lopez Aguerri, J. Alfonso, BONIFACIO, PIERCARLO, VALLENARI, Antonella, Abrams, Don Carlos, Middleton, Kevin
<b>Publisher's version (DOI)</b>	10.1117/12.2314124
<b>Handle</b>	<a href="http://hdl.handle.net/20.500.12386/28173">http://hdl.handle.net/20.500.12386/28173</a>
<b>Serie</b>	PROCEEDINGS OF SPIE
<b>Volume</b>	10706

# PROCEEDINGS OF SPIE

[SPIDigitalLibrary.org/conference-proceedings-of-spie](https://spiedigitallibrary.org/conference-proceedings-of-spie)

## WEAVE spectrograph cameras: the polishing of the spherical lenses

Izazaga, Rafael, Carrasco, Esperanza, Hidalgo, Andrea, Aguirre, Daniel, Terlevich, Elena, et al.

Rafael Izazaga, Esperanza Carrasco, Andrea Hidalgo, Daniel Aguirre, Elena Terlevich, Roberto Terlevich, Gavin Dalton, Scott Trager, J. Alfonso L. Aguerri, Piercarlo Bonifacio, Antonella Vallenari, Don Carlos Abrams, Kevin Middleton, "WEAVE spectrograph cameras: the polishing of the spherical lenses ," Proc. SPIE 10706, Advances in Optical and Mechanical Technologies for Telescopes and Instrumentation III, 107063J (10 July 2018); doi: 10.1117/12.2314124

**SPIE.**

Event: SPIE Astronomical Telescopes + Instrumentation, 2018, Austin, Texas, United States

# WEAVE spectrograph cameras: the polishing of the spherical lenses

Rafael Izazaga<sup>1,\*</sup>, Esperanza Carrasco<sup>1</sup>, Andrea Hidalgo<sup>1,2</sup>, Daniel Aguirre<sup>3,4</sup>, Elena Terlevich<sup>1</sup>, Roberto Terlevich<sup>1</sup>, Gavin Dalton<sup>2,5</sup>, Scott Trager<sup>6</sup>, J. Alfonso L. Aguerri<sup>7</sup>, Piercarlo Bonifacio<sup>8</sup>, Antonella Vallenari<sup>9</sup>, Don Carlos Abrams<sup>10</sup>, and Kevin Middleton<sup>5</sup>

<sup>1</sup>Instituto Nacional de Astrofísica, Óptica y Electrónica, Luis Enrique Erro # 1, Tonantzintla, 72840 Puebla, Mexico. <sup>2</sup>Department of Physics, University of Oxford, Keble Road, Oxford, OX1 3RH, UK. <sup>3</sup>Instituto de Ciencias Aplicadas y Tecnología, UNAM, Cd. Universitaria, Apdo. Postal 70-186, C.P. 04510, Cd. Mx. México. <sup>4</sup>Polo Universitario de Tecnología, UNAM, Vía de la Innovación No. 410, Autopista Monterrey-Aeropuerto Km. 10, PIIT C.P. 66629 Apodaca N. L., México. <sup>5</sup>RAL Space, STFC Rutherford Appleton Laboratory, Harwell Oxford, OX11 0QX, UK. <sup>6</sup>Kapteyn Institut, Rijksuniversiteit Groningen, Postbus 800, NL-9700 AV Groningen, Netherlands. <sup>7</sup>Instituto de Astrofísica de Canarias, C/Vía Láctea, s/n, E38205 La Laguna, Tenerife, Spain. <sup>8</sup>GEPI Observatoire de Paris, Place Jules Janssen, 92195 Meudon, France. <sup>9</sup>INAF, Astronomical Observatory of Padova, Vicolo dell'Osservatorio 5, 35141 Padova PD, Italy. <sup>10</sup>Isaac Newton Group of Telescopes, Calle Alvarez de Abreu 70, E-38700 Santa Cruz de La Palma, Canary Islands, Spain

\* izazagax@gmail.com

## ABSTRACT

WEAVE is the new wide field multi-object and integral field survey facility for the prime focus of the 4.2 m William Herschel Telescope. WEAVE fiber-fed spectrograph offers two resolutions,  $R \sim 5000$  and  $20,000$ . The dual-beam spectrograph has two cameras: the blue one optimized for the wavelength interval of 366 - 606 nm and the red one for 579 - 959 nm. Each camera is formed by eight lenses, one aspherical and seven spherical. The lenses of the red camera are identical to the lenses of the blue camera only differentiated by the anti-reflection coating wavelength range. The diameter of the largest surface is 320 mm while of the smallest is 195 mm. INAOE, as a member of the collaboration is responsible of the manufacturing of the 14 spherical lenses and the collimator mirror. Here, we describe the main characteristics of WEAVE high precision cameras lenses, the manufacturing challenges giving the combination of OHARA® glasses properties, dimensions and specifications. We discuss the solutions developed to achieve the very demanding specifications.

**Keywords:** optical fabrication and testing, polishing, astronomy, ground-based telescope, multi-object spectroscopy, optical design.

## 1. INTRODUCTION

WEAVE. is the new prime focus survey facility of the 4.2-m William Herschel Telescope (WHT). Within a field of view of  $2^\circ$  it will position fibers to record spectra of up to 1,000 stars and galaxies in a single exposure [1,2]. This huge leap in observing efficiency will allow astronomers to tackle several astrophysical problems [3].

The WEAVE spectrograph unit is a dual-beam and dual-resolution system with an interchangeable fiber slit input. A dichroic beam splitter divides the beam into a blue arm and red arms. The collimated beam in each beam is dispersed by a volume phase holographic (VPH) grating [4], see Figure 1. The spectrograph has two cameras, the blue one optimized for 366 - 606 nm and the red one for 579 - 959 nm wavelength intervals, respectively. Each camera is formed by eight lenses, one aspherical and seven spherical. The lenses of the red camera are identical to the lenses of the blue camera only differentiated by the anti-reflection coating wavelength range. A detailed description of the instrument

status is given by Dalton, et al. and Stuik, et al. [5,6]. The details of the 660 m diameter collimator mirror manufacturing are described in Izazaga et al. [7]. Within the WEAVE collaboration, NOVA/ASTRON is the institution responsible of the spectrograph work-package, therefore INAOE is working very closely with NOVA team.

WEAVE is now in the construction phase. In this work, we describe the specifications of WEAVE cameras lenses, being 320 mm the largest diameter while of the smallest is 195 mm, the properties of PBM2Y, PBL1Y, S-LAL9 and S-FPL51 OHARA® glasses, the manufacturing process and the final parameters of the lenses already finished. We discuss the solutions developed to achieve the very demanding requirements.

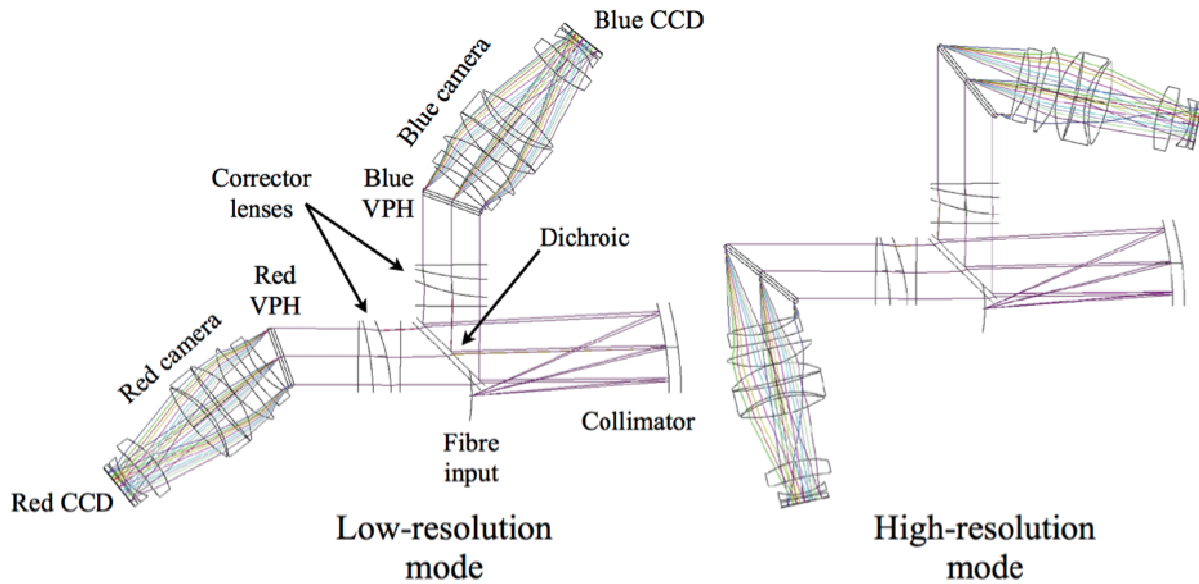


Figure 1. WEAVE optical layout, low (left) and high (right) resolution modes.

## 2. SPECIFICATIONS OF THE LENSES

For each lens, the parameters specified are radius of curvature (RoC), surface irregularity, cosmetic imperfections, surface roughness, dimensions and wedge. Table 1 shows the main parameters for each lens. Table 2 shows additional parameters including some properties of the glasses used during manufacturing processes. Table 3 are properties of OHARA® glasses.

The optical surfaces have the following specifications: 2 fringes irregularity, cosmetic imperfections of 40/20 according to MIL-13830B, 1 nm surface roughness and 2 arcmin irregularity. The recorded information and controlled parameters not included in the final reports are:

- blank revision: integrity, blank diameter, border thickness, material, manufacturer ID, photo, weight, density, flatness, parallelism, radius of curvature, surface irregularity, border angles and bubbles.
- surface manufacturing: flat tool parallelism and flatness, grinding and polishing tool characteristics, acid resistance, abrasion and density.
- cleaning: surface imperfections map, comments about stains and its removal.

Figure 2 shows a section of the manufacturing drawing of Lens 3 and 4 where the typical dimensions are specified. The blank of Blue Camera Lens 3 of 325 mm diameter and 65 mm thickness is displayed in Figure 3. Figure 4, presents the one of the Blue Camera Lens 4 of 325 mm diameter and 88 mm thickness. while in Figure 5 the blank of Red Camera Lens 6 of 265 mm diameter and 88 mm. thickness is shown. Table 4 summarizes the characteristics of the OHARA® blanks of the Red arm lenses, as measured at INAOE.

Table 1. Main parameters of the camera lenses

Element	OHARA Glass	RoC left surface (mm)	RoC right surface (mm)	Diameter (mm -0.1)	Central thickness (mm +/- 0.1)	Clear aperture left/right surface (mm)
Lens 2	PBL1Y	CX 1179.25 +/- 0.16	CX 285.16 +/- 0.01	304	62.2	298.0 / 301.0
Lens 3	S-FPL51	CX 317.75 +/- 0.01	CX 1705.64 +/- 0.32	320	59.7	316.0 / 313.0
Lens 4	PBL1Y	CC 1177.02 +/- 0.15	CC 285.09 +/- 0.01	320	32.0	310.0 / 292.0
Lens 5	S-FPL51	CX 360.69 +/- 0.01	CX 616.09 +/- 0.04	298	59.6	296.0 / 296.0
Lens 6	PBM2Y	CX 508.50 +/- 0.01	CX 794.19 +/- 0.01	160	82.3	255.0 / 234.0
Lens 7	PBM2Y	Infinite	CC 410.63 +/- 0.01	238	73.8	222.0 / 182.0
Lens 8	S-LAL9	CC 237.29 +/- 0.01	Infinite	195	20.0	172.0 / 168.6

Table 2. Glass properties considered during manufacturing.

Element	OHARA Glass	Acid resistance	Abrasion	Specific Gravity
Lens 2	PBL1Y	1.0	124	2.95
Lens 3	S-FPL51	52.1	449	3.62
Lens 4	PBL1Y	1.0	124	2.95
Lens 5	S-FPL51	52.1	449	3.62
Lens 6	PBM2Y	1.0	140	3.61
Lens 7	PBM2Y	1.0	140	3.61
Lens 8	S-LAL9	52	88	3.63

Table 3. Main properties of OHARA® glasses for WEAVE optics.

	S-FPL51	S-LAL9	PBL1Y	PBM2Y	Properties
<b>Nd</b>	1.497	1.691	1.54814	1.62004	Index of refraction
<b>Vd</b>	81.6	54.8	45.7	36.3	Abbe number
<b>Thermal properties</b>					
<b>StP (°C)</b>	-	606	361	385	Strain point
<b>AP (°C)</b>	-	630	396	418	Annealing point
<b>Tg (°C)</b>	458	653	406	436	Transformation temperature
<b>At (°C)</b>	489	679	453	470	Yield point
<b>SP (°C)</b>	-	707	567	580	Softening point
<b>Expansion coefficients (10<sup>-7</sup>/°C)</b>					
<b>-30 ~ +70°C</b>	131	61	93	86	Linear coefficients of thermal expansion
<b>+100 ~ +300°C</b>	155	74	106	97	
<b>k (W/mK)</b>	0.78	0.895	0.951	0.814	Thermal conductivity
<b>Mechanical properties</b>					
<b>E (10<sup>8</sup> N/m<sup>2</sup>)</b>	727	1075	613	571	Young modulus
<b>G (10<sup>8</sup> N/m<sup>2</sup>)</b>	280	418	252	234	Modulus of rigidity
<b>σ</b>	0.2999	0.287	0.217	0.223	Poisson ration
<b>Hk [Class]</b>	350 [4]	660 [7]	420 [4]	420 [4]	Knoop hardness
<b>Aa</b>	449	88	124	140	Abrasion
<b>d</b>	3.62	3.63	2.95	3.61	Specific gravity
<b>β (nm/cm/10<sup>5</sup> Pa)</b>	0.74	1.85	2.94	-	Photoelastic constant
<b>Chemical properties</b>					
<b>RW (P)</b>	1	2	2	2	Water resistance (Powder method).
<b>RA(P)</b>	4	5	1	1	Acid resistance (Powder method).
<b>W(S)</b>	1	2	2	1	Weathering resistance (Surface method)
<b>SR</b>	52.1	52	1	1	Acid resistance (ISO method)
<b>PR</b>	4	4	1.1	2	Phosphate resistance

Table 4. Characteristics of the blanks for the lenses of the Red arm.

Element	OHARA Glass	Diameter (mm)	Thickness (mm)	Weight (kg)
Lens 2	PBL1Y	309	68	15.04
Lens 3	S-FPL51	325	65	19.52
Lens 4	PBL1Y	325	88	21.54
Lens 5	S-FPL51	303	65	16.97
Lens 6	PBM2Y	265	88	17.52
Lens 7	PBM2Y	243	90	15.07
Lens 8	S-LAL9	200	42	5.85

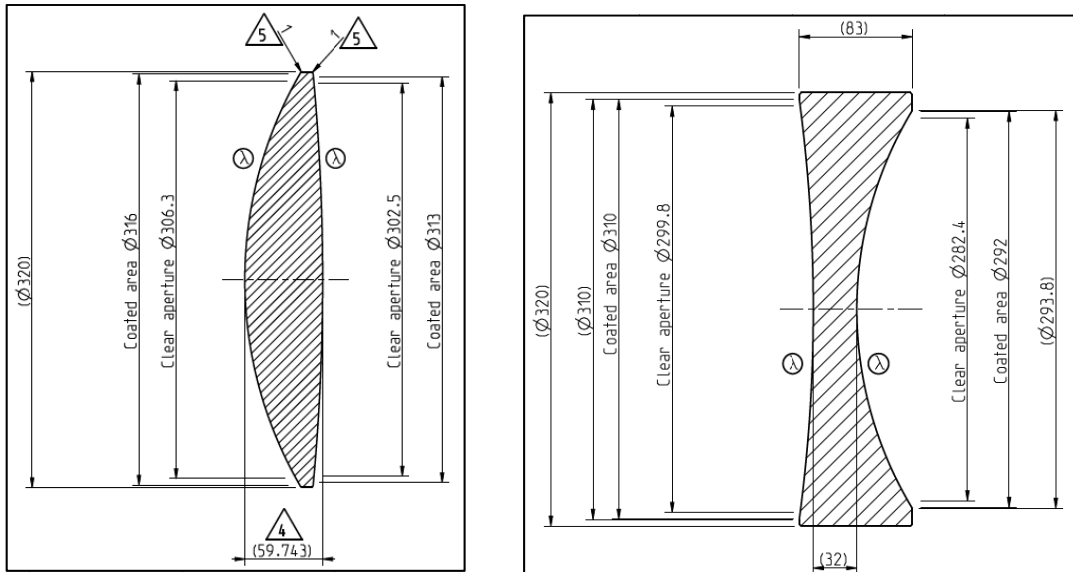


Figure 2. A section of Lenses 3 and 4 manufacturing drawings.

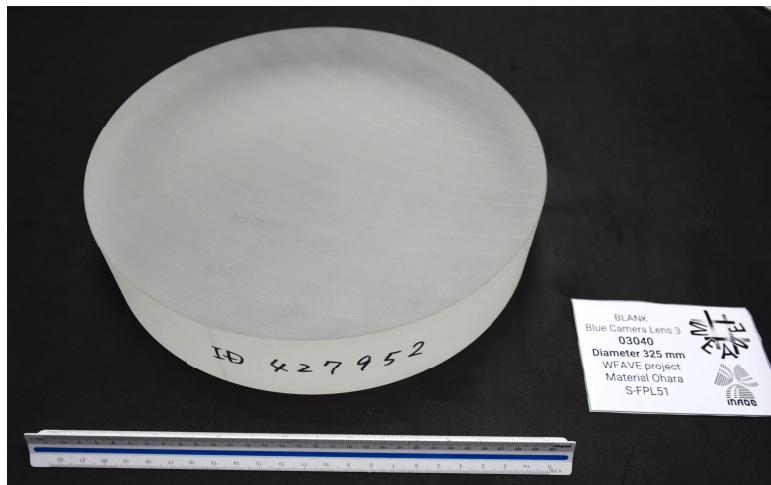


Figure 3. Blue Camera Lens 3 blank. See Table 4.

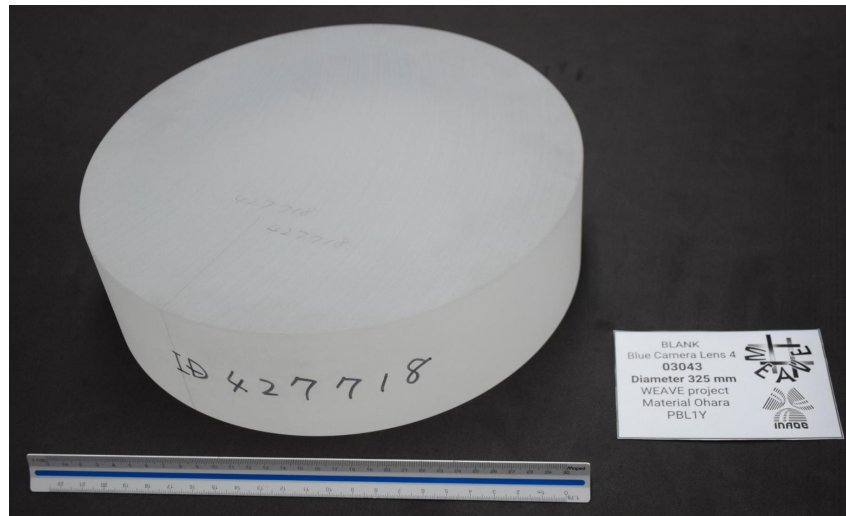


Figure 4. Blue Camera Lens 4 blank. See Table 4.



Figure 5. Red Camera Lens 6 blank. See Table 4.

### 3. MANUFACTURING PROCESS

Before starting the manufacturing process for each lens, a finite element analysis (FEA) in static mode was carried out to study the tensions and displacements of the mounting bases and the blank [8]. The goal of the simulations was to guarantee the integrity of the lens glass. To illustrate the process, we will describe Lens 4 manufacturing all along the paper. In Figure 6a we show the mesh defined for the FEA for this lens: the mesh includes a 325 mm diameter baseplate of the machine and the blank itself. The simulations include gravity and weight of the polishing tool as a static weight placed at several points in the blank surface. Considering only the effect of gravity, the maximum displacement in Z

direction (vertical) was  $12\ \mu\text{m}$ , see Figure 6b. The effect of gravity gives a considerable deformation at the borders of the lens, the displacements becomes high due to the 21.54 kg weight and the thickness of 88.25 mm of the glass. Nevertheless, the centrifugal force present on the polishing machine is enough to discard this effect, considering the weight and the thickness of the blank, and also doing the analogy with the design of a rotatory pump or a turbine, where centrifugal force helps the fluid to flow away from axis of rotation.

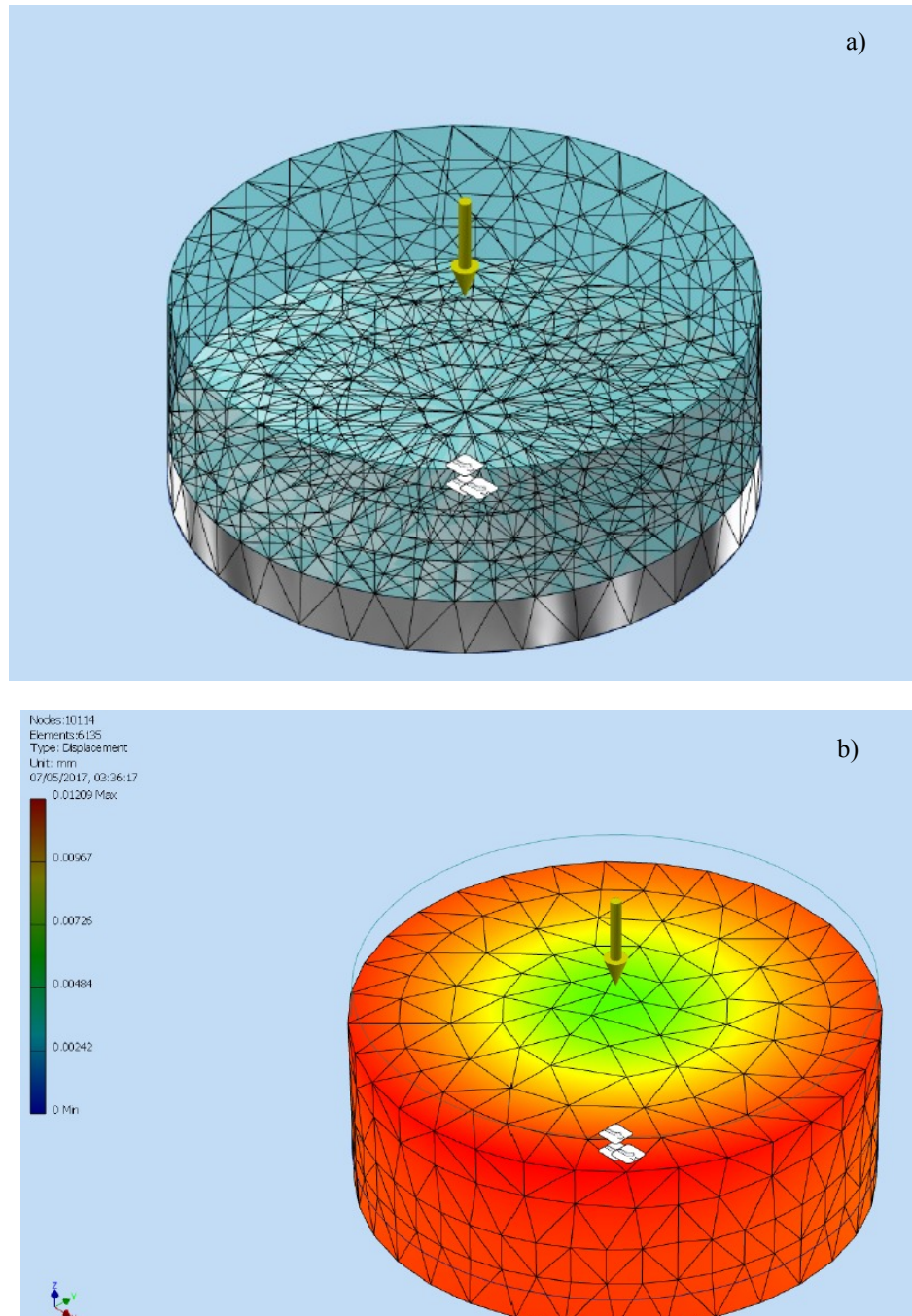


Figure 6. 3D model for Lens 4. Top: mesh considering the baseplate and the blank. The blank is shown in blue. Bottom: displacements in Z direction (vertical) where the maximum values are  $12\ \mu\text{m}$  at the borders.

### 3.1 Blocking

The polishing machine is a Strasbaugh® model 6DA-DC-4. It consists in a rotating axis to hold the blank and an overarm that holds the grinding/polishing tool. The blank of Lens 4 was placed over an aluminium plate that match its diameter of 325 mm. The blocking of the blank was carried out using wax and tape as shown in Figure 7. With these steps the blank was ready for the grinding and polishing process.

### 3.2 Curve generation

The curve generation machine is a Strasbaugh® model 7-DR, that consists in a rotating axis to hold the blank and an axis holding a diamond cup tool, see Figure 8. The cup tool selected for this process has an external diameter of 200 mm. The inclination angle of the cup tool is calculated using the following formula:

$$\theta = \sin^{-1} \left( \frac{D}{2r} \right), \quad (1)$$

where  $\theta$  is the inclination angle of the diamond cup tool,  $D$  is the diameter of the cup, in this case the external diameter and  $r$  is the radius of curvature of the lens. The speeds used in this process was 20 rpm and 1200 rpm, for the blank axis and cup axis, respectively.

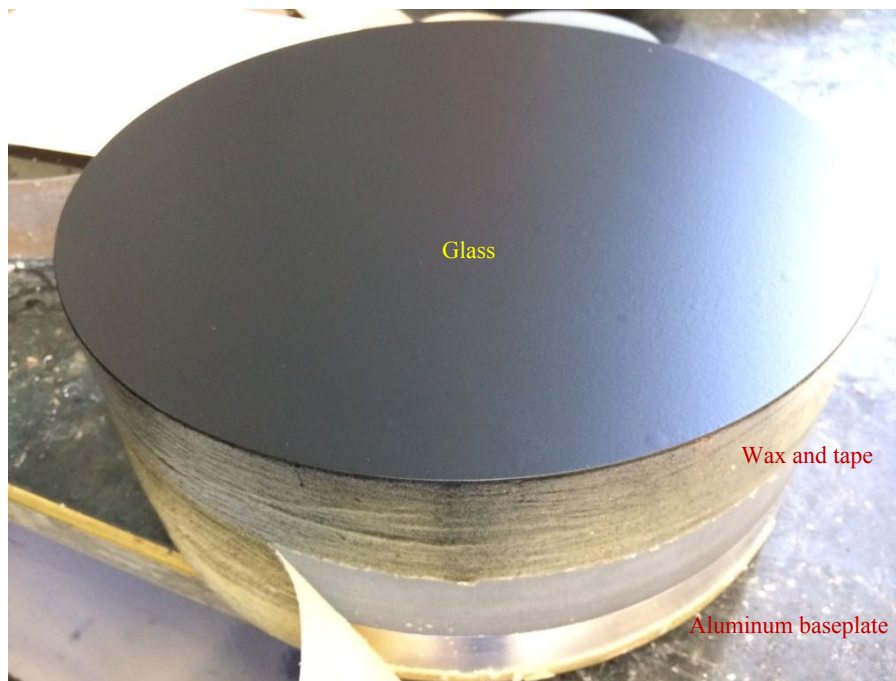


Figure 7. Blocking process of Lens 4. Diameter of 325 mm.

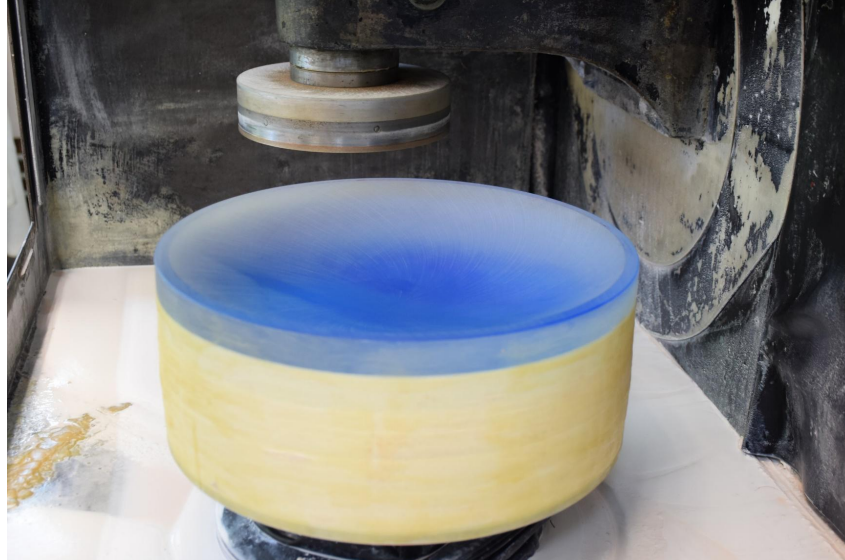


Figure 8. Curve generation process. The 200 mm diameter diamond cup is on top of Lens 4.

### 3.3 Grinding and polishing

The polishing and grinding processes were carried out in the Strasbaugh® 6DA-DC-4 machine. In this machine a rotating axis holds the lens and an oscillating arm holds a glass tool maintaining loose abrasive between both surfaces. Microgrit® WCA (Aluminum oxide) was used in the grinding process with stages of 40, 25, 15 and 5 microns as average particle size (APS). In the middle of the process a visual inspection was carried out to verify the smoothness of every stage. Figure 9 shows a moment during the grinding process; the lens and the glass tool can be appreciated. The speeds used were 10 rpm for the rotating axis and 4 rpm for the overarm. This process last about a week per surface.

The polishing process was carried out using a pitch polishing tool (pitch #450 Universal Photonics Inc.), see Figure 10. The polishing compound selected was Hastilite® RS (Cerium oxide) 0.5 microns APS. All grinding abrasives and polishing compounds are from Universal Photonics Inc. The polishing process last about a month per surface, depending on the glass characteristics, as explained below.

PBL1Y has a well behavior during polishing, in other words, a fast grinding time, approximately 30 minutes per abrasive stage and easy correction of the figure during polishing process i.e. irregularity doesn't change during polishing at a low material removal rate. However, its low abrasion value of 124, see Table 3, was indicative that it was going to be time consuming to reach the RoC for fast surfaces. This was the case for Lens 4 with a CC RoC of 285.09 mm and 320 mm diameter. The RoC was corrected at a rate of 0.01 mm per hour while the irregularity value remains under specification.

PBM2Y has the particularity of thermal effects during polishing due to the friction between the glass and tool. This might be due to the material composition and/or the glass fabrication process as this effect hasn't been observed in a similar glass Schott® F2. Nevertheless, PBM2Y offers advantages over F2 as better transmission in the blue wavelength interval. The effect was also present during optical testing, as the irregularity figure varied with the room temperature: we measured 2 fringes of irregularity at 20 °C but 3 fringes at 22 °C. Therefore, we carried out the irregularity measurement 24 hr. after the polishing process ended, at a room temperature of 20 °C +/- 0.4. Stains were common to appear under humid conditions and became worse when relative humidity was about 80%. To avoid this problem a room dehumidifier was used at INAOE optical testing laboratory

S-LAL9 has the highest specific gravity of 3.63 and the lowest abrasion value of 88. The combination of these properties diffculted to accomplish the CC 237.29 mm RoC of Lens 8: The RoC correction was performed at the same rate as Lens 4 i.e. 0.01mm per hour. Due to its acid resistance of 5, see Table 3, stains appeared during polishing and became worse when a polished surface was in contact with the aluminum baseplate under humid conditions. The stains appeared even in a clean and dry environment while the lens was covered with a high quality protective coat (Pre-cote #33 from Universal Photonics®).

S-FPL51 was the most difficult to polish. This is due to its low index of refraction of 1.497, the high abrasion value of 449 and low Knoop hardness of 350, similar to a crystal, see Table 3. It presented thermal effects during polishing as in the case of PBM2Y but with a worse thermal effect during testing. Several scratches appeared during the grinding process. Due to its abrasion value - the highest of WEAVE glasses- the material removal rate was high, approximately 0.05 mm per hour, measured in thickness. To avoid scratches during grinding, 9T microns abrasive was used instead of the usual 5 microns. Hastilite® RS was used during the first two hours of polishing providing a low removal rate while diminishing small scratches. In the rest of the process BaikaloX® 0.05 microns polishing compound was used to obtain the final figure correction with a low removal rate without compromising the thickness of the lens.



Figure 9. Grinding process for left surface of Lens 4. Note the glass tool over the workpiece.



Figure 10. Polishing process. Note the pitch tool over the workpiece.

## 4. OPTICAL TESTING

### 4.1 Irregularity measurements

Irregularity measurements were particularized for each surface. The irregularity measurements were carried out using a Zygo® Fizeau type interferometer. We accomplish a full aperture interferometry test for the concave surfaces of lenses 4, 7 and 8, using a  $f/0.65$  reference sphere ( $PV=\lambda/20$ ,  $\lambda=632.8$  nm Zygo® Corp.), as illustrated in Figure 11.

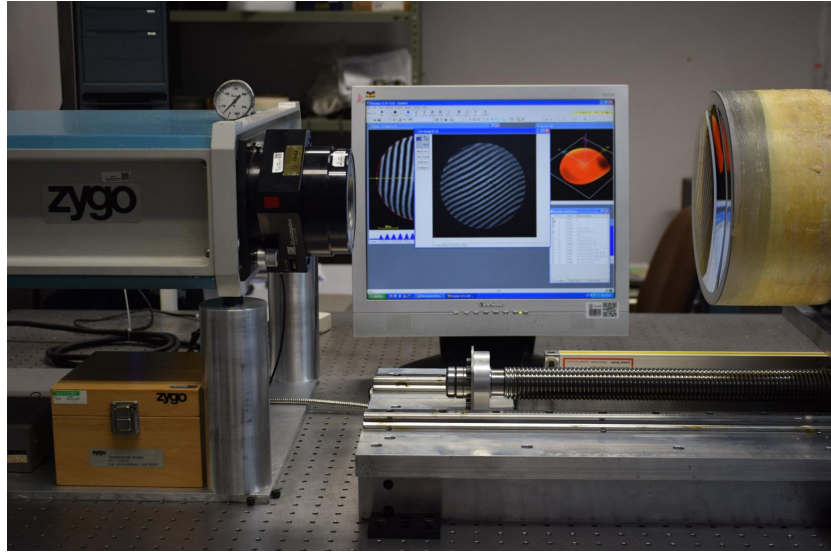


Figure 11. Experimental set-up to measure irregularity of concave surfaces. A reference sphere that produce a  $f/0.65$  beam illuminates the complete surface under test.

Newton interferometer was used to test the convex and flat surfaces. Eight reference surfaces were designed and fabricated at INAOE for testing the convex surfaces of lenses 2, 3, 5 and 6. A detailed description of the design and characteristics of these reference test plates is given by Hidalgo et al. [9]. A reference flat (Edmund Optics® 304.8 mm diameter,  $PV=\lambda/20$ ) was used to test flat surfaces of lenses 7 and 8. Given the diameters of the lenses the convex and flat surfaces were tested by sub-apertures. The irregularity of the complete aperture was obtained by applying the sub-aperture stitching technique [10]. Figure 12 shows the Newton interferometer set-up used to test convex and flat surfaces.

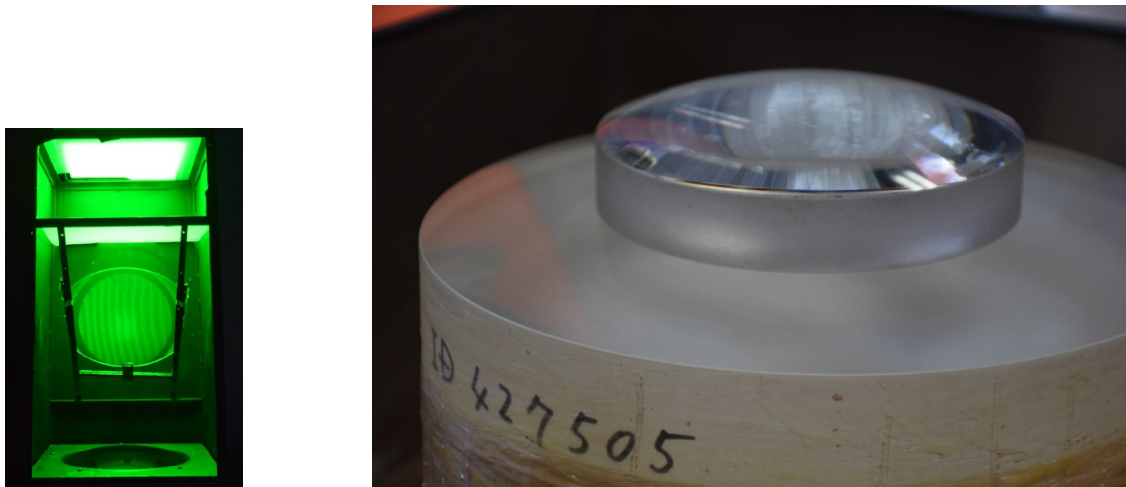


Figure 12. Left: Newton interferometer test set-up. Right: Lens 6 sub-aperture measurement.

## 4.2 Interferogram analysis

For concaves surfaces a phase shifting Fizeau-type interferometer was used. The interferograms obtained with the set-up described were analyzed using Durango® software (Diffraction International Inc.). In this configuration nine interferograms were obtained in one stepping capture by using a piezoelectric placed at the reference sphere mount. Figure 13 and 14 show the interferograms and its irregularity values for Lens 4 right and Lens 8 left surfaces, respectively.

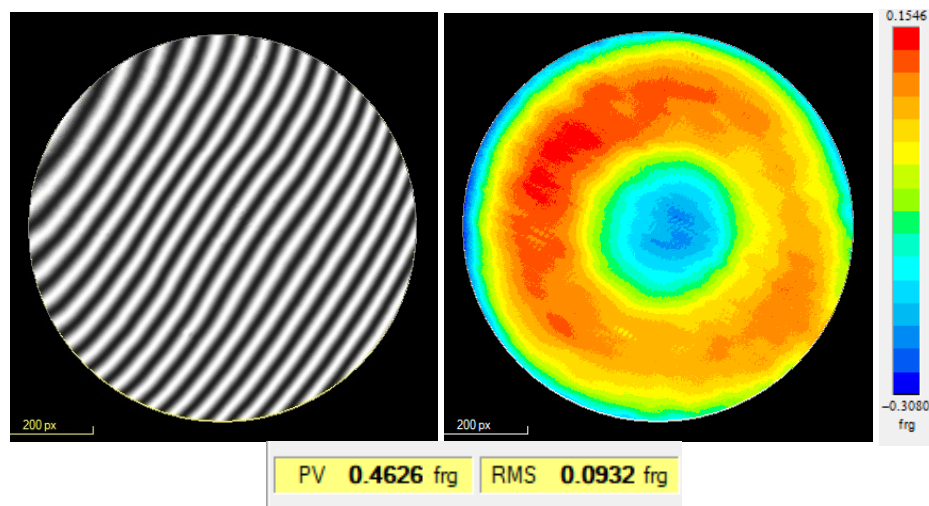


Figure 13. Irregularity obtained for Lens 4 right surface.

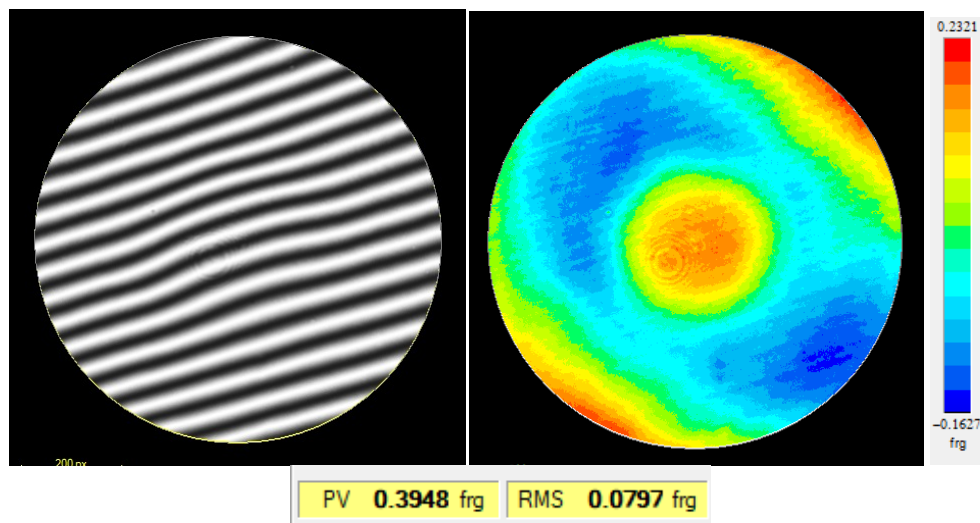


Figure 14. Irregularity obtained in Lens 8 left surface.

For convex surfaces a sub-aperture stitching method [10] was applied. Nine sub-apertures, a central one and eight located at the edge of the surface were obtained. Each individual subaperture interferogram was analyzed using Durango® interferometry software as well. The complete aperture analysis of the nine subapertures is performed using a

software developed at INAOE. Figures 15 and 16 show the interferograms and irregularity values obtained for the left surfaces of Lens 2 and Lens 6.

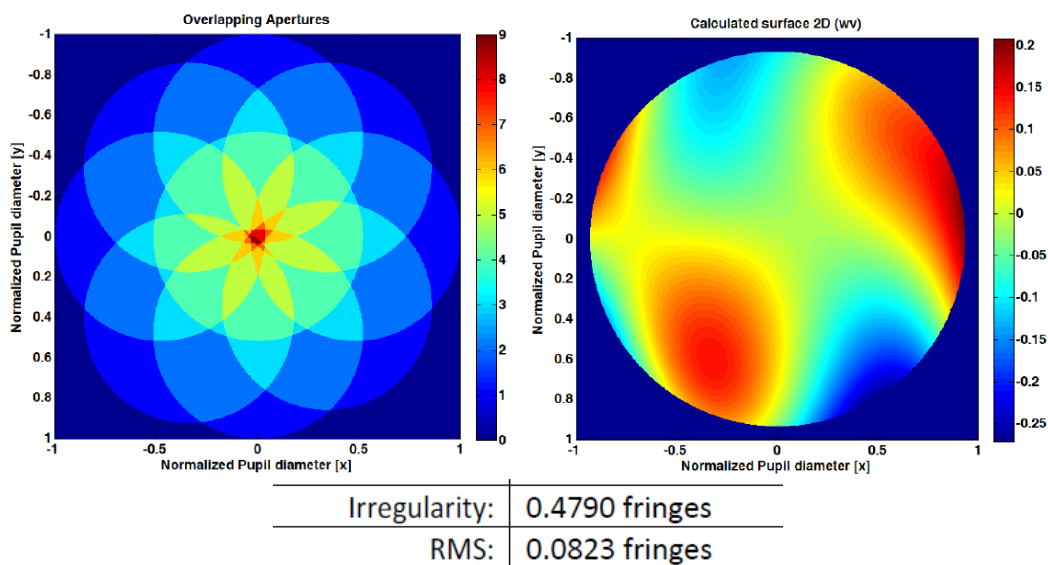


Figure 15. Subaperture Stitching analysis of Lens 2 left surface.

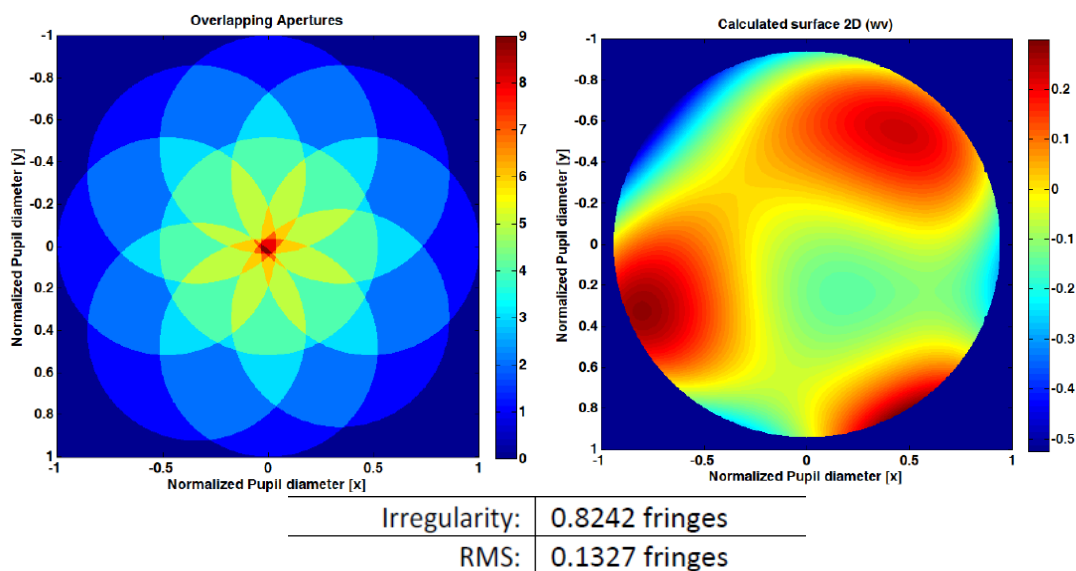


Figure 16. Subaperture Stitching analysis of Lens 6 left surface.

## 5. RESULTS

We present the parameters measurements for the Red arm lenses finished at the time of writing this paper. In Table 5 a summary of Lens 2 manufacturing results is presented, Table 6 is the summary corresponding to Lens 4, Table 7 the results for Lens 6, Table 8 the results for Lens 7 and Table 9 the measurements of Lens 8. The first and second columns correspond to each parameter and its specified value. In the third column, we report the values measured and in the

fourth the instrument and/or method used for the measurement. Figures 17 and 18 shows lenses 4 and 8 during the final packing processes, respectively.

Table 5. Specifications and final measurements of Lens 2.

Red camera Lens 2 summary				
<b>NOVA Reference</b>	03038			
<b>Part Name</b>	Red camera Lens 2			
<b>Glass</b>	Ohara PBL1Y	<b>ID</b>	427717	
<b>Parameter</b>	<b>Specification</b>	<b>Measurement</b>	<b>Measurement</b>	<b>Instrument or method</b>
Left surface		Test plate	Left surface	
RoC (mm)	CX 1179.259+/- 0.01687	1179.336	-	Via test plate RoC (Oriel slide optical bench +/- 0.01 mm)
Irr in clear aperture	2 fr	0.0545	0.479	Newton interferometer Subaperture stitching
MIL 13830 SD	40/20	-	20/10	Visual inspection vs. calibrated reference (Bryson optical 7641896)
Protective chamfer (mm)	0.5-1.5 x 45°	-	1.3	Mitutoyo Caliper +/-0.01 mm
Right surface		Test plate	Right surface	
RoC (mm)	CX 285.164+/- 0.0088	285.161	-	Via test plate RoC (slide optical bench +/- 0.005mm)
Irr in clear aperture	2 fr	0.2816	1.254	Newton interferometer Subaperture stitching
MIL 13830 SD	40/20	-	10/10	Visual inspection vs. calibrated reference (Bryson optical 7641896)
Protective chamfer	0.5-1.5 x 45°	-	1.3	Mitutoyo Caliper +/-0.01 mm
Lens			Lens	
Edge diameter (mm)	304 +0.0/-0.1		303.96	Mitutoyo Caliper +/-0.01 mm
Central thickness (mm)	62.254+/-0.1		62.08	Mitutoyo Height Caliper +/- 0.01 mm
Wedge (arcmin)	2		0.167	Mitutoyo Dial Indicator +/-0.001 mm

Table 6. Specifications and final measurements of Lens 4.

Red camera Lens 4 summary			
<b>NOVA Reference</b>	03044		
<b>Part Name</b>	Red camera Lens 4		
<b>Glass</b>	Ohara PBL1Y	427933	
<b>Parameter</b>	<b>Specification</b>	<b>Measurement</b>	<b>Instrument or method</b>
Left surface		Left surface	
RoC (mm)	CC 1177.026 +/- 0.15	1176.97	Oriel Slide optical bench (+/- 0.01mm), five measurements average
Irr in clear aperture	2 fr	0.3872	Zygo Mark II interferometer full aperture (Reference sphere f/0.65, PV= $\lambda$ /20)
MIL 13830 SD	40/20	10/10	Visual inspection vs. calibrated reference (Brysen optical 7641896)
Protective chamfer (mm)	1-2 x 45°	1.2	Mitutoyo Caliper +/-0.01 mm
Right surface		Right surface	
RoC (mm)	CC 285.091+/-0.01	285.105	Zygo Mark II interferometer (slide optical bench +/- 0.005mm), five measurements average
Irr in clear aperture	2 fr	0.4626	Zygo Mark II interferometer full aperture (Reference sphere f/0.65, PV= $\lambda$ /20)
MIL 13830 SD	40/20	10/5	Visual inspection vs. calibrated reference (Brysen optical 7641896)
Protective chamfer	1-2 x 45°	1.2	Mitutoyo Caliper +/-0.01 mm
Lens		Lens	
Edge diameter (mm)	320 +0.0/-0.1	319.99	Mitutoyo Caliper +/-0.01 mm
Central thickness (mm)	32+/-0.1	32.01	Mitutoyo Height Caliper +/- 0.01 mm
Wedge (arcmin)	2	0.159	Mitutoyo Dial Indicator +/-0.001 mm

Table 7. Specifications and final measurements of Lens 6.

Red camera Lens 6 summary				
<b>NOVA Reference</b>	03050			
<b>Part Name</b>	Red camera Lens 6			
<b>Glass</b>	Ohara PBM2Y	<b>ID</b>	427505	
<b>Parameter</b>	<b>Specification</b>	<b>Measurement</b>	<b>Measurement</b>	<b>Instrument or method</b>
Left surface		Test plate	Left surface	
RoC (mm)	CX 508.5018+/-0.01	508.501	-	Via test plate RoC (slide optical bench +/- 0.005mm)
Irr in clear aperture	2 fr	0.1721	0.8242	Newton interferometer Subaperture stitching
MIL 13830 SD	40/20	-	20/10	Visual inspection vs. calibrated reference (Brysen optical 7641896)
Protective chamfer (mm)	1-2 x 45°	-	1.3	Mitutoyo Caliper +/-0.01 mm
Right surface		Test plate	Right surface	
RoC (mm)	CX 794.1924+/-0.01	794.133	-	Via test plate RoC (slide optical bench +/- 0.005mm)
Irr in clear aperture	2 fr	0.2692	1.1031	Newton interferometer Subaperture stitching
MIL 13830 SD	40/20	-	10/10	Visual inspection vs. calibrated reference (Brysen optical 7641896)
Protective chamfer	1-2 x 45°	-	1.3	Mitutoyo Caliper +/-0.01 mm
Lens			Lens	
Edge diameter (mm)	260 +0.0/-0.1		259.99	Mitutoyo Caliper +/-0.01 mm
Central thickness (mm)	82.3+/-0.1		81.66	Mitutoyo Height Caliper +/-0.01 mm
Wedge (arcmin)	2		0.198	Mitutoyo Dial Indicator +/-0.001 mm

Table 8. Specifications and final measurements of Lens 7.

Red camera Lens 7 summary			
<b>NOVA Reference</b>	03053		
<b>Part Name</b>	Red camera Lens 7		
<b>Glass</b>	Ohara PBM2Y	427508	
<b>Parameter</b>	<b>Specification</b>	<b>Measurement</b>	<b>Instrument or method</b>
Left surface		Left surface	
RoC (mm)	Infinite	-	Edmund optics Ø152mm reference flat (PV= $\lambda$ /20)
Irr in clear aperture	2 fr	0.7576	Newton interferometer Subaperture stitching
MIL 13830 SD	40/20	20/20	Visual inspection vs. calibrated reference (Brysen optical 7641896)
Protective chamfer (mm)	1-2 x 45°	1.3	Mitutoyo Caliper +/-0.01 mm
Right surface		Right surface	
RoC (mm)	CC 410.631+/-0.01	410.634	Zygo interferometer (slide optical bench +/- 0.005mm)
Irr in clear aperture	2 fr	0.2923	Zygo interferometer / Full aperture
MIL 13830 SD	40/20	10/10	Visual inspection vs. calibrated reference (Brysen optical 7641896)
Protective chamfer	1-2 x 45°	1.2	Mitutoyo Caliper +/-0.01 mm
Lens		Lens	
Edge diameter (mm)	238 +0.0/-0.1	237.98	Mitutoyo Caliper +/-0.01 mm
Central thickness (mm)	73.76+/-0.1	73.74	Mitutoyo Height Caliper +/- 0.01 mm
Wedge (arcmin)	2	0.217	Mitutoyo Dial Indicator +/-0.001 mm

Table 9. Specifications and final measurements of Lens 8.

Red camera Lens 8 summary			
NOVA Reference	03056		
Part Name	Red camera Lens 8		
Glass	Ohara S-LAL9	427739	
Parameter	Specification	Measurement	Instrument or method
Left surface		Left surface	
RoC (mm)	CC 237.288	237.282	Interferometer / Slide optical bench (+/- 0.005mm),
Irr in clear aperture	2 fr	0.3948	Zygo interferometer / full aperture
MIL 13830 SD	40/20	20/10	Visual inspection vs. calibrated reference (Brysen optical 7641896)
Protective chamfer (mm)	1-2 x 45°	1.2	Mitutoyo Caliper +/-0.01 mm
Right surface		Right surface	
RoC (mm)	Infinite	-	Edmund optics reference flat (Ø=203.2mm)
Irr in clear aperture	2 fr	0.4828	Newton interferometer / full aperture
MIL 13830 SD	40/20	20/10	Visual inspection vs. calibrated reference (Brysen optical 7641896)
Protective chamfer	1-2 x 45°	1.2	Mitutoyo Caliper +/-0.01 mm
Lens		Lens	
Edge diameter (mm)	195 +0.0/-0.1	194.98	Mitutoyo Caliper (+/-0.01 mm)
Central thickness (mm)	20 +/-0.1	19.94	Mitutoyo Height Caliper (+/- 0.01 mm)
Wedge (arcmin)	2	0.26	Mitutoyo Dial Indicator (+/-0.001 mm)

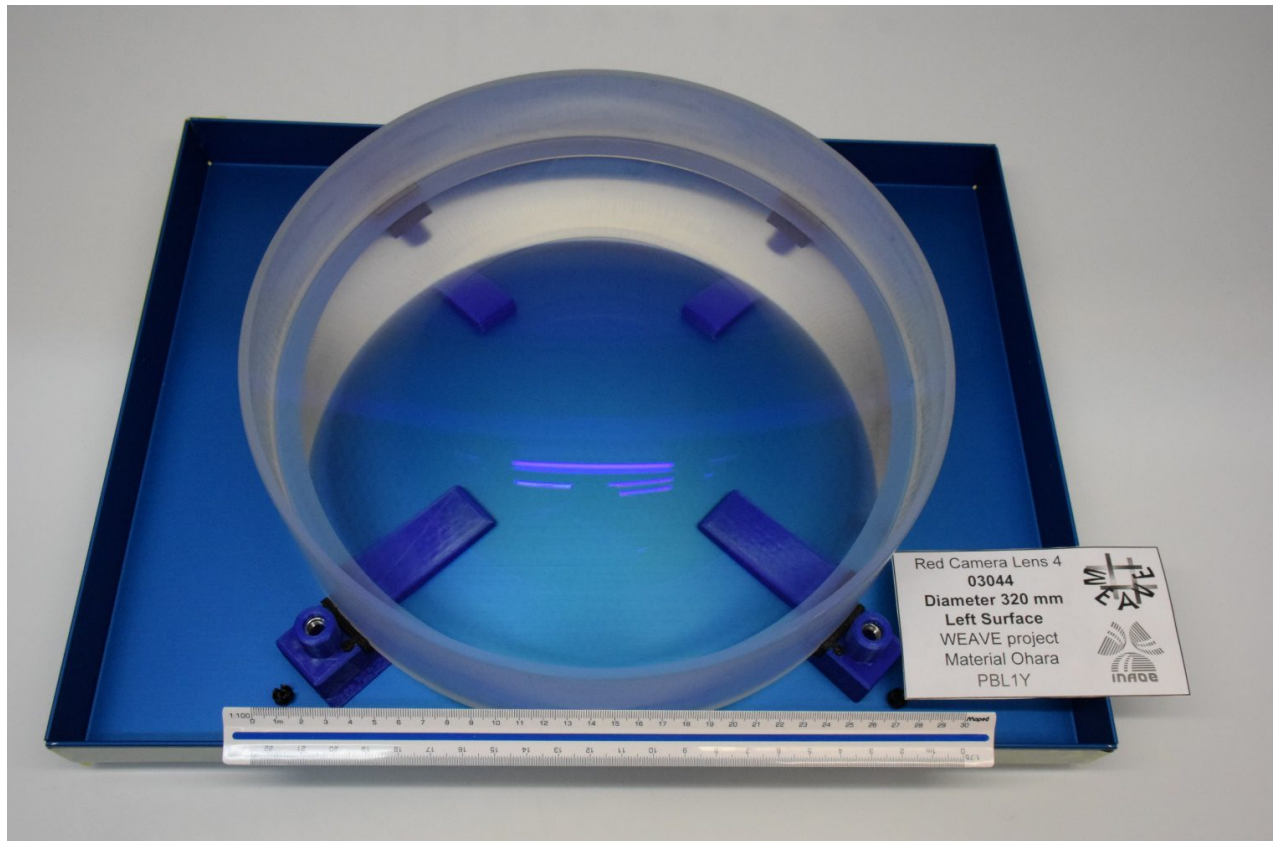


Figure 17. Red Camera Lens 4.

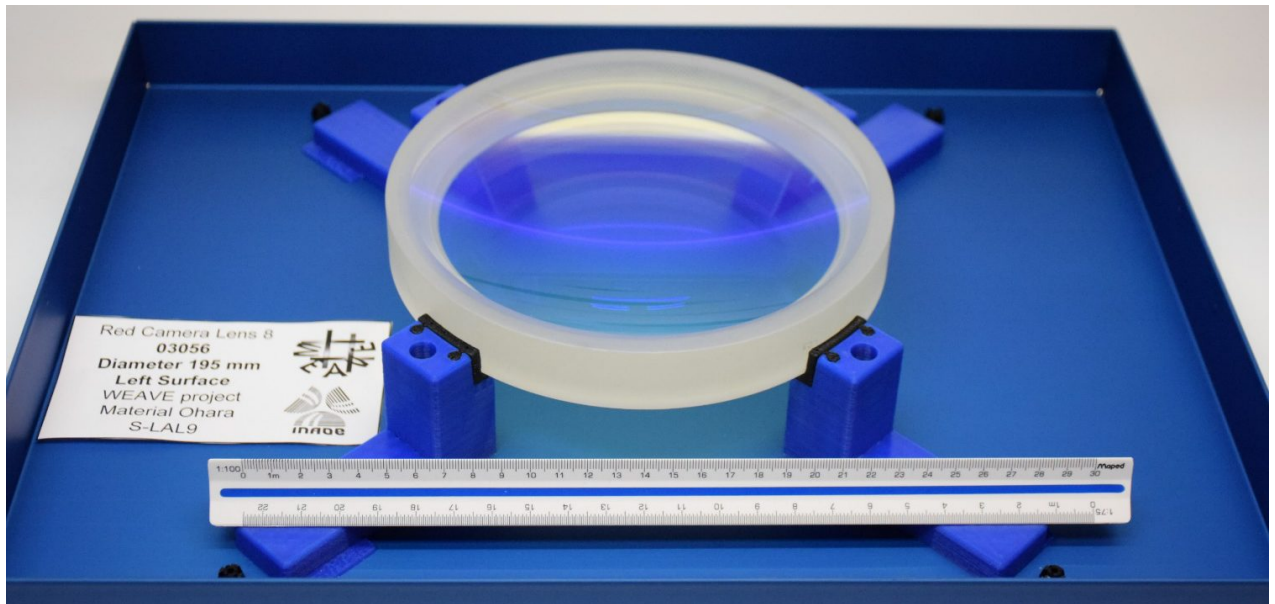


Figure 18. Red Camera Lens 8.

## 6.- CONCLUSIONS

The manufacturing process of WEAVE camera lenses represents a challenge as it is unique optics. The specifications were very demanding given the diameters of the lenses and the glasses properties. Additionally, the geometry of the bevels in lenses 7 and 8 and the thickness in lenses, 4, 6 and 7 required extreme care. FEA simulations were carried out to ensure the manufacturability within acceptable time and risks. The different processes and solutions involved in the manufacturing were described. The methodology to measure the optical parameters was presented. The data summary of each lens prove that the lenses fulfill all the requirements showing INAOE capabilities to manufacture very high quality unique elements. Regarding the, red arm Lens 4, 6, 7 and 8 are already in NOVA. Lens 2 is completely finished and packed. Lens 3 and 5 are in stand by for centering. Regarding the blue arm Lens 2 was polished at CIO. The manufacturing of the other 7 lenses is in progress at INAOE.

## ACKNOWLEDGEMENT

The authors thank José Miguel Arroyo, Valentín López, Magdalena Hernández, Javier Arriaga, José Armando de la Luz, Gloria Jaimes, Jorge Reyes, Araceli Huepa and Alfonso Salas, personnel of INAOE Optical Fabrication and Testing Laboratory their valuable work and effort during the manufacturing of WEAVE optics.

## REFERENCES

- [1] Dalton, G. et al., "WEAVE: the next generation wide-field spectroscopy facility for the William Herschel telescope". Proc. SPIE **8446**, pp. 84460P (2012).
- [2] Rogers, K. et al. "The design of the WEAVE spectrograph", Proc. SPIE **9147**, pp. 91476H, (2014).
- [3] Dalton, G. et al., "Project overview and update on WEAVE: the next generation wide-field spectroscopy facility for the William Herschel Telescope", Proc. SPIE **9147**, pp. 91470L (2014).
- [4] Dalton, G. et al., "Final design and progress of WEAVE: the next generation wide-field spectroscopy facility for the William Herschel Telescope," Proc. SPIE **9908**, pp. 99081G (2016).
- [5] Dalton, G. et al., "Construction progress of WEAVE: the next generation wide-field spectroscopy facility for the William Herschel Telescope". Proc. SPIE **10702**, pp. 10702-47, (2018).
- [6] Stuijk, R. et al., "Integration and testing of the WEAVE Spectrograph", Proc. SPIE **10702**, pp. 10702-275, (2018).
- [7] Izazaga, R., et al. "The polishing of WEAVE spectrograph collimator mirror", Proc. SPIE **10706**, pp. 10706-18, (2018).
- [8] Hidalgo, A., "Camera lenses and collimator mirror optics manufacturing for the WEAVE Spectrograph", MSc. thesis, INAOE, Mexico, (2017).
- [9] Hidalgo, A., et al., "Test-plate design and manufacturing for the camera lenses of the WEAVE spectrograph", Proc. SPIE **10706**, pp. 10706-130, (2018).
- [10] Aguirre, D. et al. "MEGARA Optics: Sub-aperture Stitching Interferometry for Large Surfaces", PASP **130**, 045001, (2018).